

# Laser-Ablation FTICR Mass Spectrometry of Metal Sulfides: Gaseous Anionic $[\text{Ni}_x\text{S}_y]^-$ Clusters

John H. El Nakat,<sup>†</sup> Ian G. Dance,<sup>\*,†</sup> Keith J. Fisher,<sup>\*,†</sup> Dennis Rice,<sup>‡</sup> and Gary D. Willett<sup>†</sup>

Contribution from the School of Chemistry, University of New South Wales, P.O. Box 1, Kensington, NSW 2033, Australia, and the Mineral Resources Development Laboratory, NSW Department of Minerals and Energy, P.O. Box 76, Lidcombe, NSW 2141, Australia.

Received September 24, 1990

**Abstract:** Laser (Nd/YAG, 1064 nm) ablation of  $\text{Ni}_3\text{S}_2$  or  $\text{NiS}$ , monitored by Fourier transform ion cyclotron resonance mass spectrometry, yields at least 28  $[\text{Ni}_x\text{S}_y]^-$  ions, ranging from  $[\text{NiS}]^-$  to  $[\text{Ni}_{15}\text{S}_{10}]^-$ . The  $x,y$  combinations are 1,1; 1,2; 1,3; 2,2; 2,3; 3,2; 3,3; 4,4; 4,5; 5,4; 6,4; 6,5; 7,5; 7,6; 8,5; 8,6; 8,7; 9,6; 9,7; 10,7; 10,8; 11,7; 11,8; 12,7; 12,8; 12,11; 13,8; 15,10.  $[\text{Ni}_2\text{S}_2]^-$  and  $[\text{Ni}_3\text{S}_4]^-$  are unaffected by collisions with argon at  $2 \times 10^{-7}$  mbar, while the ions  $[\text{NiS}_2]^-$ ,  $[\text{Ni}_3\text{S}_3]^-$ , and  $[\text{Ni}_4\text{S}_4]^-$  decompose in ca 0.05 s under the same conditions. Evidence for isomeric ions with differing reactivities could be obtained for  $[\text{Ni}_3\text{S}_3]^-$ , but sensitivity limitations precluded reactivity measurements for larger ions. Geometrical structures are postulated for all ions, based on established structural principles, and correspond in many cases to the structures of condensed phase clusters, devoid of terminal ligands.

## Introduction

We are using laser-ablation Fourier transform ion cyclotron resonance (LA-FTICR) mass spectrometry to investigate metal chalcogenide complexes in the gas phase. One impetus for this research originates in the many molecular clusters with chalcogenido-polymetallate cores that have recently been prepared and characterized in the crystalline state.<sup>1</sup> Examples of these molecules are  $[\text{Ni}_9\text{S}_9(\text{PET}_3)_6]^{2+}$ ,<sup>2</sup>  $[\text{Ni}_{15}\text{S}_{15}(\text{PPh}_3)_6]^{3-}$ ,<sup>3</sup>  $[\text{M}_6\text{S}_{17}]^{4-}$  ( $\text{M} = \text{Nb}, \text{Ta}$ ),<sup>4</sup>  $[\text{Ni}_{34}\text{Se}_{22}(\text{PPh}_3)_{10}]^{5-}$ ,<sup>5</sup>  $[\text{S}_4\text{Cd}_{17}(\text{SPh})_{28}]^{2-}$ ,<sup>6</sup>  $[\text{Na}_2\text{Fe}_{18}\text{S}_{30}]^{8-}$ ,<sup>7</sup>  $[\text{SNi}_8(\text{SBU}^+)_9]^-$ ,<sup>8</sup>  $[\text{Ni}_{20}\text{Te}_{18}(\text{PET}_3)_{12}]^{9-}$ ,<sup>9</sup>  $[\text{Cu}_{29}\text{Se}_{15}(\text{PPR}^+)_3]_{12}$ , and  $[\text{Cu}_{36}\text{Se}_{18}(\text{PBU}^+)_3]_{12}$ .<sup>10</sup> It appears that many chalcogenido-polymetallate molecules must possess considerable thermodynamic stability, at least when they are associated with appropriate terminal ligands which may not be chalcogenide. In addition to these polymetallic molecules with precisely defined structures, there are metal chalcogenide clusters that occur over a wide size range and have ill-defined structure. These include many colloidal metal sulfides that have been prepared in and stabilized by a variety of media that inhibit or prevent aggregation and growth.<sup>11-13</sup> The biological generation of nanocrystallites  $\text{Cd}_x\text{S}_y(\gamma\text{-EC})_z$  of diameter ca. 20 Å has recently been described.<sup>14</sup>

Laser-ablation mass spectrometry<sup>15</sup> could elucidate metal chalcogenide clusters in two ways. One derives from the structural congruence of many molecular metal sulfide clusters with sections of nonmolecular metal chalcogenide lattices.<sup>16</sup> Structurally, the macromolecular clusters are fragments of the nonmolecular solid state. For example, the  $\text{M}_8\text{S}_8\text{L}_8$  and  $\text{M}_6\text{S}_6\text{L}_6$  clusters occur as such, but with intercluster connections, in the pentlandite series of minerals and the Chevrel phases.<sup>17</sup> Similarly, the  $\text{Fe}_6\text{S}_6\text{L}_6$  clusters<sup>18</sup> are a section of the vallerite lattice;  $[\text{V}_4\text{S}_2(\text{SCH}_2\text{CH}_2\text{S})_6]^{2-}$ <sup>19</sup> is related to the  $\text{LiVS}_2$  phases; and the  $[\text{E}_4\text{M}_{10}(\text{SR})_{16}]^{4-}$  clusters ( $\text{E} = \text{S}, \text{Se}$ ;  $\text{M} = \text{Zn}, \text{Cd}$ )<sup>20</sup> are symmetrical fragments of the sphalerite (zinc blende) lattice. Therefore it is pertinent to investigate whether molecular fragments might be liberated from congruent nonmolecular solids upon deposition of the appropriate energy.

Second, laser ablation can generate *elemental* ions, which can then combine or react with neutrals to generate cluster ions.<sup>21,22</sup> Thus there exists the possibility of synthesizing metal chalcogenide cluster ions in the laser generated plasma at the surface of a solid.<sup>23</sup> Using isotope-labeled samples, Linton et al.<sup>22</sup> have demonstrated that Ni and S ions combine to generate small  $[\text{Ni}_x\text{S}_y]^+$  species upon laser ablation of  $\text{NiS}$ , or of S plus Ni.

The advantage of FTICR mass spectrometry is that ions generated in the ionization process can be trapped in the ICR cell

and their properties and reactivities investigated further.<sup>24-34</sup> Nickel is a significant metal for investigation of gas-phase

- (1) (a) Dance, I. G. *Polyhedron* 1986, 5, 1037. (b) Fenske, D.; Ohmer, J.; Hachgenel, J.; Nerzweiler, K. *Angew. Chem., Int. Ed. Engl.* 1988, 27, 1277-1296. (c) Dance, I. G. In *Comprehensive Coordination Chemistry*; Wilkinson, G., Gillard, R. D., McCleverty, J. A., Eds.; Pergamon Press: Oxford, 1987, Chapter 4. (d) Müller, A.; Diemann, E. *Adv. Inorg. Chem.* 1987, 31, 89.
- (2) Cecconi, F.; Ghilardi, C. A.; Midollini, S. *Inorg. Chem.* 1983, 22, 3802.
- (3) Hong, M.; Huang, Z.; Liu, H. J. *Chem. Soc., Chem. Commun.* 1990, 1210.
- (4) Sola, J.; Do, Y.; Berg, J. M.; Holm, R. H. *J. Am. Chem. Soc.* 1983, 105, 7784.
- (5) Fenske, D.; Ohmer, J.; Hachgenel, J. *Angew. Chem., Int. Ed. Engl.* 1985, 24, 993.
- (6) Lee, G. S. H.; Craig, D. C.; Ma, I.; Scudder, M. L.; Bailey, T. D.; Dance, I. G. *J. Am. Chem. Soc.* 1988, 110, 4863.
- (7) You, J.-F.; Snyder, B. S.; Papefthymliou, G. C.; Holm, R. H. *J. Am. Chem. Soc.* 1990, 112, 1067.
- (8) Kruger, T.; Krebs, B.; Henkel, G. *Angew. Chem., Int. Ed. Engl.* 1989, 28, 61.
- (9) Brennan, J. G.; Siegrist, T.; Stuczynski, S. M.; Steigerwald, M. L. *J. Am. Chem. Soc.* 1989, 111, 9240.
- (10) Fenske, D.; Krautscheid, H.; Balter, S. *Angew. Chem., Int. Ed. Engl.* 1990, 29, 796.
- (11) Fendler, J. H. *Chem. Rev.* 1987, 87, 877.
- (12) Steigerwald, M. L.; Brus, L. E. *Annu. Rev. Mater. Sci.* 1989, 19, 471.
- (13) Herron, N.; Wang, Y.; Eckert, H. *J. Am. Chem. Soc.* 1990, 112, 1322.
- (14) (a) Dameron, C. T.; Reese, R. N.; Mehra, R. K.; Kortan, A. R.; Carroll, P. J.; Steigerwald, M. L.; Brus, L. E.; Winge, D. R. *Nature* 1989, 338, 596. (b) Dameron, C. T.; Smith, B. R.; Winge, D. R. *J. Biol. Chem.* 1989, 264, 17355. (c) Dameron, C. T.; Winge, D. R. *Inorg. Chem.* 1990, 29, 1343.
- (15) *Lasers and Mass Spectrometry*; Lubman, D. M., Ed.; Oxford University Press: New York, 1989.
- (16) Dance, I. G. In preparation.
- (17) (a) Burdett, J. K.; Miller, G. J. *J. Am. Chem. Soc.* 1987, 109, 4081. (b) Chevrel, R.; Hirrien, M.; Sergent, M. *Polyhedron* 1986, 5, 87.
- (18) (a) Coucouvanis, D.; Salifoglou, A.; Kanatzidis, M. G.; Dunham, W. R.; Sliopoulos, A.; Kostikas, A. *Inorg. Chem.* 1988, 27, 4066. (b) Kanatzidis, M. G.; Hagen, K. S.; Dunham, W. R.; Lester, R. K.; Coucouvanis, D. *J. Am. Chem. Soc.* 1985, 107, 953. (c) Coucouvanis, D.; Kanatzidis, M. G.; Dunham, W. R.; Hagen, K. S. *J. Am. Chem. Soc.* 1984, 106, 7998.
- (19) Christou, G.; Money, J. K.; Huffman, J. C. *J. Am. Chem. Soc.* 1987, 109, 2210.
- (20) Dance, I. G.; Choy, A.; Scudder, M. L. *J. Am. Chem. Soc.* 1984, 106, 6285.
- (21) McElvany, S. W.; Cassady, C. J. *J. Phys. Chem.* 1990, 94, 2057.
- (22) (a) Musselman, I. H.; Linton, R. W.; Simons, D. S. *Anal. Chem.* 1988, 60, 110. (b) Linton, R. W.; Musselman, I. H.; Bruynseels, F.; Simons, D. S. In *Microbeam Analysis*; Gelss, R. H., Ed.; San Francisco Press: San Francisco, CA, 1987; p 365.
- (23) Dance, I. G.; El Nakat, J. H.; Fisher, K. J.; Willett, G. D. *Inorg. Chem.* In press.
- (24) Comisarow, M. B. *Adv. Mass Spectrom.* 1980, 8, 1698.
- (25) Wanczek, K. P. *Int. J. Mass Spectrom. Ion Proc.* 1984, 60, 11.

<sup>†</sup> University of New South Wales.

<sup>‡</sup> NSW Department of Minerals and Energy.

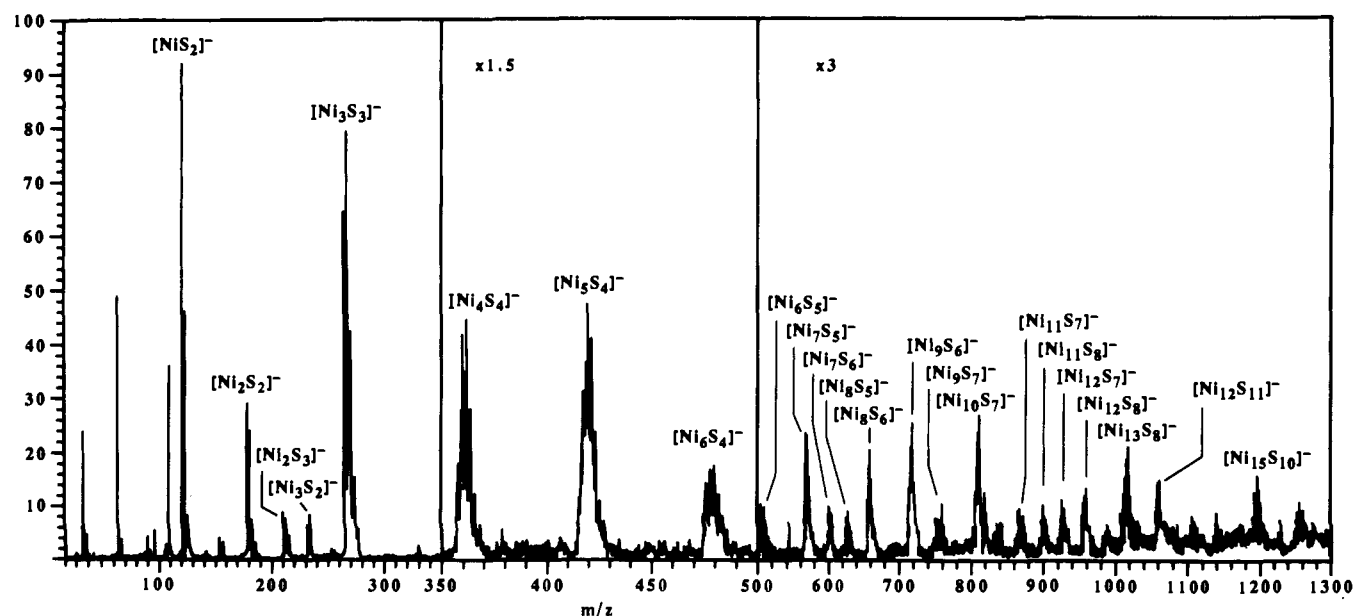


**Figure 1.** Composite broad-band, negative ion spectra of  $\text{Ni}_3\text{S}_2$  when laser-ablated (1064 nm) with a Q-switched pulse of ca.  $1600 \text{ MW cm}^{-2}$ . The higher mass sections are recorded with sensitivities increased by 1.5 and 3 as marked.

chalcogenide clusters, because the number and variety of molecular nickel chalcogenide clusters known in the condensed phases are greater than those of other metals. In this paper we report our studies with  $\text{Ni}_3\text{S}_2$  (the mineral heazlewoodite) and  $\text{NiS}$ . The solid-state structure of  $\text{Ni}_3\text{S}_2$  is three-dimensionally nonmolecular:<sup>35,36</sup> each Ni is surrounded by four S atoms at 2.27 Å, in tetrahedral array, and is also bonded to four Ni at 2.51, 2.52 Å; each S is surrounded by six Ni at 2.27 Å. As we shall describe below, this structure is composed of  $[\text{Ni}_3\text{S}_2]$  entities linked in an almost cubic lattice.

### Experimental Section

The nickel sulfide sample was prepared as a button by reaction of nickel powder (2.1 g, 36 mmol) and sulfur (1.5 g, 47 mmol of S) in a fusion mixture of lithium borax glass (70 g), sodium carbonate (35 g), quartz powder (20 g), and magnesium oxide (10 g). After 2 h at  $1000^\circ\text{C}$  and cooling for 30 min, the button (2.5 g) was easily separated. The identification as  $\text{Ni}_3\text{S}_2$  was by X-ray diffraction, with characteristic  $d$  spacings at 4.08, 2.87, 2.42, 2.04, 1.83, 1.82, 1.66 Å (ASTM 2-772).

The mass spectra were obtained with a Spectrospin CMS-47 (FT-ICR) mass spectrometer, equipped with a 4.7 T superconducting magnet.<sup>37</sup> Fragments of the button were secured onto a satellite probe tip or were pressed into a 2 mm thick layer on a detachable cylindrical (5-mm radius) probe tip. These were then introduced, using a direct insertion probe, into the ICR cell. A cylindrical ICR cell (30 mm radius  $\times$  60 mm) with six titanium single section plates was used in an ultra-high-vacuum chamber maintained at a base pressure of  $10^{-9}$  mbar by a turbomolecular pump.<sup>38</sup>

Laser-ablation of the solid sample was performed with a Nd/YAG laser (1064 nm, Spectra Physics DCR-11) focused on an area of 0.01  $\text{mm}^2$  of the sample at the end of the cell, flush and in contact with the ICR trapping plate. Two laser irradiance modes were used. In the

Q-switched mode the pulse width was  $\sim 8$  ns, producing a maximum energy of  $\sim 1600 \text{ MW cm}^{-2}$  at the sample. Neutral density filters were used to modify the pulse energy at the sample. In the long pulse mode the flash lamp fired and the system was opened to allow the emergence of a  $\sim 230$ - $\mu\text{s}$  pulse with a total energy equal to that of the Q-switched pulse. The peak energy at the sample produced in this mode was  $\sim 0.72 \text{ MW cm}^{-2}$ . The energy of the pulses at the sample surface was measured ( $\pm 10\%$ ) with a power meter (Genetec ED-500).

Ions were trapped in the cell by a potential of  $-4$  V (for negative ions,  $+4$  V for positive ions). Broad and narrow band modes<sup>38</sup> were operated with the following sequence of events: (i) a quench rf pulse and a short delay preceded the ionizing laser pulse; (ii) after a variable delay (often 3  $\mu\text{s}$ ) the rf pulse for ion excitation was applied; (iii) the signal acquisition was initiated 500  $\mu\text{s}$  after the excitation pulse. The acquisition time was set to a maximum according to the desired mass window.

In a typical collisional activation (CA) experiment<sup>39,40</sup> the pulse sequence was as follows: (i) a quench pulse, followed by a short delay, followed by the ionizing laser pulse; (ii) the rf pulse to eject all unwanted ions occurred 3  $\mu\text{s}$  later; (iii) the ion selected for observation was activated and then allowed to undergo collisions with argon at a pressure of  $2 \times 10^{-7}$  mbar, for a variable reaction time of up to 20 s; and (iv) the rf pulse for ion excitation was applied and the signal acquired as above. The (MS)<sup>n</sup> experiments were carried out with a loop that repeated the ejection and ion activation pulses ( $n - 1$ ) times before detection.

### Results

**Ions Observed.** Laser ablation of  $\text{Ni}_3\text{S}_2$  with the spectrometer operating in the positive ion mode yielded only  $\text{Ni}^+$ . However, rich spectra were obtained in the negative ion mode. Figure 1 shows broad-band negative ion spectra for  $\text{Ni}_3\text{S}_2$  ablated by using the Q-switched laser with ca.  $1600 \text{ MW cm}^{-2}$ . The ions are listed in Table I, together with the ions produced by a filtered Q-switched pulse of  $150 \text{ MW cm}^{-2}$  and a long pulse of ca.  $0.72 \text{ MW cm}^{-2}$ . All ions were identified by narrow band experiments and simulation of the isotopomer profile, as illustrated in Figure 2.

We note the following characteristics of this set of ions. The larger ions are obtained only with the maximum laser irradiance. Independent of laser power, the most abundant ion is  $[\text{NiS}_2]^-$ , the ion  $[\text{Ni}_3\text{S}_3]^-$  is consistently strong, and the ion  $[\text{Ni}_3\text{S}_2]^-$  is consistently weak. The compositions of the observed ions are graphed in Figure 3. In all except three small ions ( $[\text{NiS}_2]^-$ ,  $[\text{NiS}_3]^-$ ,  $[\text{Ni}_2\text{S}_3]^-$ ) the number of S atoms is not greater than the

- (26) Gross, M. L.; Rempel, D. L. *Science* **1984**, *226*, 261.  
 (27) Freiser, B. S. In *Techniques in Ion-Molecule Reactions*; Farrar, J. M., Saunders, W. H., Eds.; Wiley: New York, 1989, pp 61-118.  
 (28) Marshall, A. G. *Acc. Chem. Res.* **1985**, *18*, 316.  
 (29) Wilkins, C. L.; Chowdhury, A. K.; Nuwaugir, L. M.; Coates, M. L. *Mass Spectrom. Rev.* **1989**, *8*, 67.  
 (30) Russell, D. H. *Mass Spectrom. Rev.* **1986**, *5*, 167.  
 (31) Marshall, A. G. In *Adv. Mass Spectrom.* **1989**, *11A*, 651-668.  
 (32) Sharpe, P.; Richardson, D. E. *Coord. Chem. Rev.* **1989**, *93*, 59.  
 (33) Irlon, M. P.; Selinger, A.; Wendel, R. *Int. J. Mass Spectrom. Ion Proc.* **1990**, *96*, 27.  
 (34) Marshall, A. G.; Verdun, F. R. In *Fourier Transforms in NMR, Optical and Mass Spectrometry, a Users Handbook*; Elsevier: Amsterdam, 1989.  
 (35) Westgren, A. Z. *Anorg. Allg. Chem.* **1938**, *239*, 82.  
 (36) Fleet, M. E. *Am. Mineral.* **1977**, *62*, 341.  
 (37) Allemann, M.; Kellerhals, Hp.; Wanczek, K. P. *Int. J. Mass Spectrom. Ion Proc.* **1983**, *46*, 139.

- (38) Greenwood, P. F.; Strachan, M. G.; Willett, G. D.; Wilson, M. A. *Org. Mass Spectrosc.* **1990**, *25*, 353.  
 (39) (a) Jacobson, D. F.; Freiser, B. S. *J. Am. Chem. Soc.* **1983**, *105*, 736.  
 (b) Jacobson, D. B.; Freiser, B. S. *J. Am. Chem. Soc.* **1983**, *105*, 7484.  
 (40) Hop, C. E. C. A.; McMahon, T. B.; Willett, G. D. *Int. J. Mass Spectrom. Ion Proc.* **1990**, *101*, 191.

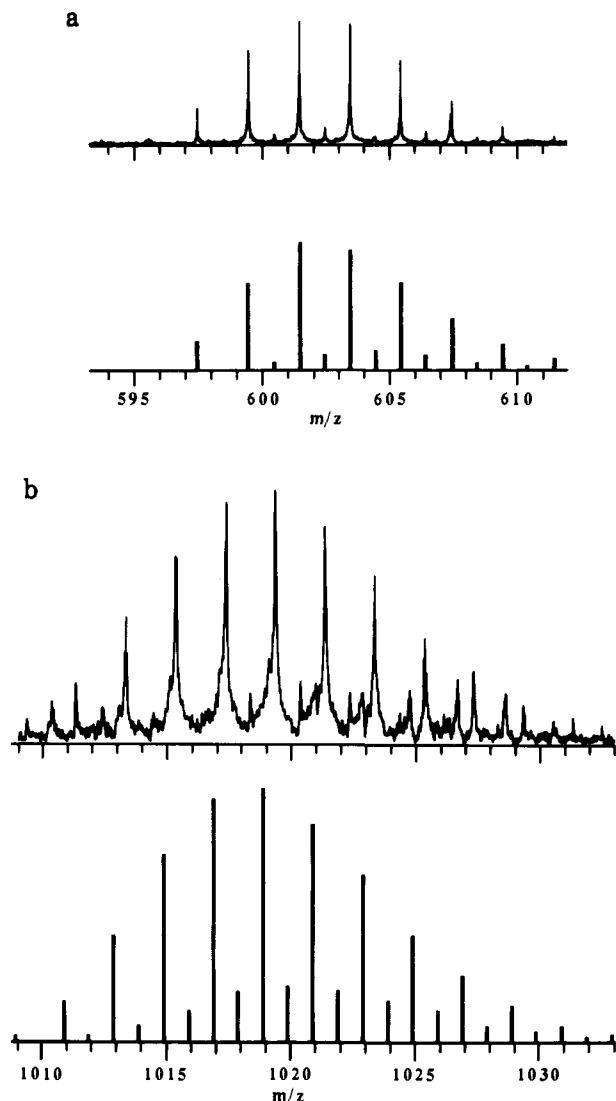


**Figure 2.** Narrow band spectra of the ions (a)  $[\text{Ni}_7\text{S}_6]^-$  and (b)  $[\text{Ni}_{13}\text{S}_8]^-$ , together with the calculated isotopomer intensity distributions. The additional weak peaks centered around  $m/z$  1027 in spectrum b are not positively identified, but they may be due to  $[\text{Ni}_{11}\text{S}_{12}]^-$ . The experimental mass calibration error in part b is 0.4.

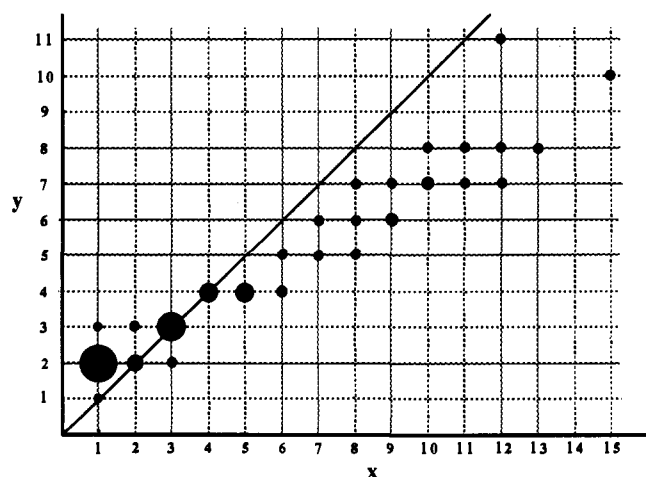


**Figure 3.** Compositions and relative abundances of the  $[\text{Ni}_x\text{S}_y]^-$  ions, with reference to the equiatomic composition  $x = y$ . The sizes of the circles are approximately proportional to the ion intensities.

number of Ni atoms. Various sequences of ions are apparent, as is the absence of several ions that would be consistent with these series. The most notable absence is  $[\text{Ni}_4\text{S}_3]^-$ : indeed there is an apparent differentiation of the seven ions in the array (see Figure

**Table I.** Negative Ions Observed in the Laser-Ablation FTICR Mass Spectrum of  $\text{Ni}_3\text{S}_2$

$m/z^a$	composition	relative intensity		
		1600 MW $\text{cm}^{-2}$	150 MW $\text{cm}^{-2}$	0.72 MW $\text{cm}^{-2}$
31.97	$[\text{S}]^-$	6		
63.94	$[\text{S}_2]^-$	50	12	28
89.91	$[\text{NiS}]^-$	5	7	<5
95.92	$[\text{S}_3]^-$	6	7	30
121.9	$[\text{NiS}_2]^-$	100	100	100
153.9	$[\text{NiS}_3]^-$	5	<5	16
179.8	$[\text{Ni}_2\text{S}_2]^-$	32	32	10
211.8	$[\text{Ni}_2\text{S}_3]^-$	9	13	<5
239.8	$[\text{Ni}_3\text{S}_2]^-$	<5	<5	<5
271.7	$[\text{Ni}_3\text{S}_3]^-$	86	81	34
361.6	$[\text{Ni}_4\text{S}_4]^-$	33	32	6
421.6	$[\text{Ni}_5\text{S}_4]^-$	35	41	
479.5	$[\text{Ni}_6\text{S}_4]^-$	12	11	
511.5	$[\text{Ni}_6\text{S}_5]^-$	6	7	
569.4	$[\text{Ni}_7\text{S}_5]^-$	9	11	
601.4	$[\text{Ni}_7\text{S}_6]^-$	<5	7	
629.3	$[\text{Ni}_8\text{S}_5]^-$	<5	11	
661.3	$[\text{Ni}_8\text{S}_6]^-$	7		
693.3	$[\text{Ni}_8\text{S}_7]^-$	<5		
719.3	$[\text{Ni}_9\text{S}_6]^-$	10		
751.2	$[\text{Ni}_9\text{S}_7]^-$	<5		
811.2	$[\text{Ni}_{10}\text{S}_7]^-$	10		
843.1	$[\text{Ni}_{10}\text{S}_8]^-$	<5		
869.1	$[\text{Ni}_{11}\text{S}_7]^-$	<5		
901.1	$[\text{Ni}_{11}\text{S}_8]^-$	<5		
927.0	$[\text{Ni}_{12}\text{S}_7]^-$	<5		
959.0	$[\text{Ni}_{12}\text{S}_8]^-$	5		
1018.9	$[\text{Ni}_{13}\text{S}_8]^-$	8		
1054.9	$[\text{Ni}_{12}\text{S}_{11}]^-$	5		
1200.8	$[\text{Ni}_{15}\text{S}_{10}]^-$	5		

<sup>a</sup> For the most intense isotopomer.

3) from  $[\text{NiS}]^-$  to  $[\text{Ni}_3\text{S}_3]^-$  from the remainder in the array from  $[\text{Ni}_4\text{S}_4]^-$  to  $[\text{Ni}_{13}\text{S}_8]^-$ . A search for  $[\text{Ni}_4\text{S}_3]^-$  provided no evidence that it is formed in our experiments; however the nonobservation of most ions with  $x > 14$ ,  $y > 8$  is a consequence of the loss of sensitivity in this high-mass region, and such ions may be formed by our laser ablation technique.

In general the Ni/S ratio ( $x/y$ ) in the observed ions is about 1.35, ranging from 1 to 1.7 (disregarding the smallest ions). Indeed there are various series of ions which progress by addition of the formula  $\text{Ni}_3\text{S}_2$ . For instance, the set of ions  $[\text{Ni}_x\text{S}_2]^-$  ( $x = 1, 2, 3$ ) add  $\text{Ni}_3\text{S}_2$  to give the set  $[\text{Ni}_x\text{S}_4]^-$  ( $x = 4, 5, 6$ ), with similar progression to  $[\text{Ni}_x\text{S}_6]^-$  ( $x = 7, 8, 9$ ), and then to  $[\text{Ni}_x\text{S}_8]^-$  ( $x = 10, 11, 12$ ):  $[\text{Ni}_{15}\text{S}_{10}]^-$  is also a member of this progression. Another instance is the addition of  $\text{Ni}_3\text{S}_2$  to  $[\text{Ni}_x\text{S}_5]^-$  ( $x = 6, 7, 8$ ) to give  $[\text{Ni}_x\text{S}_7]^-$  ( $x = 9, 10, 11$ ). Within the array of ions there are also sequences which correspond to addition of NiS.

To explore the influence of the composition and structure of the solid sample on the ions obtained by this technique we investigated NiS and mixtures of Ni with sulfur (plastic allotrope). The broad-band spectrum of NiS is very similar to that of  $\text{Ni}_3\text{S}_2$ , although with less intensity, but there is an additional ion  $[\text{Ni}_4\text{S}_5]^-$  in the spectrum of NiS. Experiments with elemental Ni and S were limited by the vapor pressure of sulfur and yielded only polysulfide ions  $[\text{S}_6]^-$  and  $[\text{S}_8]^-$ .

**Collisional Activation Experiments.** Collisional activation (CA) experiments could be effected only for the more abundant ions,  $[\text{NiS}_2]^-$ ,  $[\text{Ni}_2\text{S}_2]^-$ ,  $[\text{Ni}_3\text{S}_3]^-$ ,  $[\text{Ni}_4\text{S}_4]^-$ , and  $[\text{Ni}_5\text{S}_4]^-$ . The most stable ions in the presence of argon at  $2 \times 10^{-7}$  mbar were  $[\text{Ni}_2\text{S}_2]^-$  and  $[\text{Ni}_5\text{S}_4]^-$ : there was <10% diminution of intensity of  $[\text{Ni}_2\text{S}_2]^-$  during 15 s, and no daughter ions were detected. Similarly,  $[\text{Ni}_5\text{S}_4]^-$ , the largest ion that could be studied under CA conditions with argon, decomposed <10% to  $[\text{Ni}_3\text{S}_3]^-$  during 20-s collision time. In contrast,  $[\text{NiS}_2]^-$ ,  $[\text{Ni}_3\text{S}_3]^-$ , and  $[\text{Ni}_4\text{S}_4]^-$  when undergoing collisions with argon under the same conditions each dissociated with a half-life of ca. 0.05 s to smaller ions.

CA studies of  $[\text{Ni}_3\text{S}_3]^-$  gave  $[\text{Ni}_2\text{S}_2]^-$ ,  $[\text{NiS}_2]^-$ , and  $[\text{NiS}]^-$  as the principal daughter ions, as shown graphically in Figure 4. The

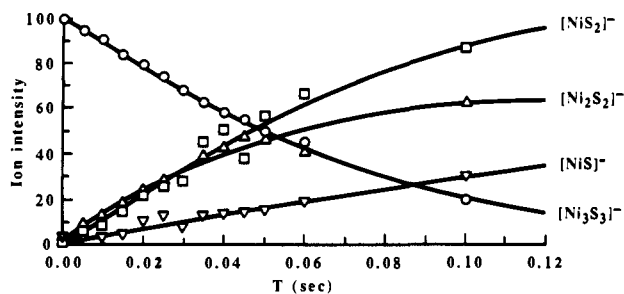


**Figure 4.** The decay and growth of anions in the collisional activation of  $[\text{Ni}_3\text{S}_3]^-$ : the ion intensities are relative and have not been normalized.

CA of  $[\text{Ni}_4\text{S}_4]^-$ , occurring at about the same rate as that shown for  $[\text{Ni}_3\text{S}_3]^-$  in Figure 4, produced  $[\text{Ni}_3\text{S}_3]^-$  as the principal ion. The CA of  $[\text{Ni}_2\text{S}_2]^-$ , also at a similar rate, yielded  $[\text{NiS}]^-$ ,  $[\text{S}_2]^-$ , and  $[\text{S}]^-$ .

**Mass Spectrometry of Isolated Ions.** The course of the dissociation of  $[\text{Ni}_4\text{S}_4]^-$  was investigated also by tandem mass spectrometry, (MS)<sup>n</sup>, in which daughter ions were isolated in the cell in vacuo and their FT mass spectra measured after subsequent activation. When  $[\text{Ni}_3\text{S}_3]^-$  was isolated as the daughter ion of  $[\text{Ni}_4\text{S}_4]^-$ , it dissociated to  $[\text{NiS}_2]^- + [\text{S}_3]^- + [\text{S}_2]^- + [\text{S}]^-$ . This was different from the CA of  $[\text{Ni}_3\text{S}_3]^-$ , and thus two different dissociation pathways are available to the ion  $[\text{Ni}_3\text{S}_3]^-$ , dependent on its origin. When derived directly from the laser ablation and subject to collisional activation with argon the products were  $[\text{Ni}_2\text{S}_2]^-$ ,  $[\text{NiS}_2]^-$ ,  $[\text{NiS}]^-$ ,  $[\text{S}_2]^-$ , and  $[\text{S}]^-$ , while when the  $[\text{Ni}_3\text{S}_3]^-$  was trapped as the daughter of  $[\text{Ni}_4\text{S}_4]^-$ , its dissociation yielded  $[\text{NiS}_2]^-$ ,  $[\text{S}_3]^-$ ,  $[\text{S}_2]^-$ , and  $[\text{S}]^-$ , with  $[\text{Ni}_2\text{S}_2]^-$  significantly absent. It is probable that there are two ions  $[\text{Ni}_3\text{S}_3]^-$ , differing in structure and energy. For reasons of insufficient sensitivity it has not yet been possible for us to investigate the possibility that other larger  $[\text{Ni}_x\text{S}_y]^-$  ions possess isomers.

## Discussion

By laser ablation of solid nickel sulfides  $\text{Ni}_3\text{S}_2$  and  $\text{NiS}$  we have uncovered a new set of  $[\text{Ni}_x\text{S}_y]^-$  ions, of which at least some possess considerable stability. The fact that the set of  $[\text{Ni}_x\text{S}_y]^-$  ions formed is largely independent of the chemical composition of the sample ablated indicates that the ions are formed in the laser induced plasma adjacent to the solid surface and are not necessarily released as such from the solid.<sup>23</sup> The larger S/Ni ratio in solid  $\text{NiS}$  is reflected in the formation of one additional sulfur-excessive gaseous ion,  $[\text{Ni}_4\text{S}_5]^-$ , not observed for  $\text{Ni}_3\text{S}_2$ . Laser ablation of nickel metal under our conditions yields few measurable anions, and we surmise that the sulfur, present as  $[\text{S}_n]^-$  ions, is desirable to intercept  $\text{Ni}_m$  neutrals formed in the laser ablation.

Larger  $[\text{Ni}_x\text{S}_y]^-$  ions are obtained with more powerful laser pulses. The plasma density increases with the power of the laser pulse (the pressure surge in the spectrometer increases with the laser pulse power), and consequently the denser plasmas produced by more powerful pulses will allow more associative collisions. It is also possible that larger fragments of the solid are directly excited with the more powerful pulses: we cannot differentiate these two possible mechanisms. The ions we observe contain more atoms than any gas-phase transition-metal chalcogenide ions previously reported.<sup>41-44</sup>

The investigation of the same solids ( $\text{Ni}_3\text{S}_2$  and  $\text{NiS}$ ) by Linton,<sup>45</sup> using a lower power laser microprobe mass analyzer, yielded the seven ions in the subset with  $n \leq 3$  (Figure 4) but did not

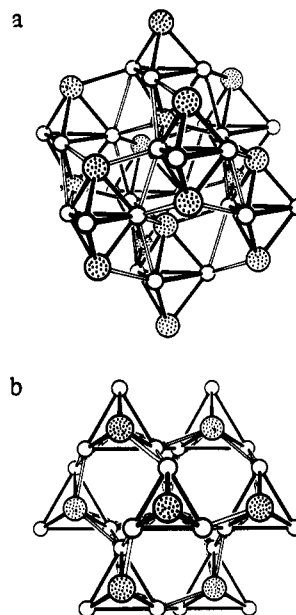


**Figure 5.** Representations of the crystal structure of  $\text{Ni}_3\text{S}_2$ ; bonds within the  $\text{Ni}_3\text{S}_2$  trigonal bipyramids are drawn filled, those connecting them are open: dotted circles are S atoms. (a) The pseudocubic array (drawn with the 3-fold axis almost vertical) of  $\text{Ni}_3\text{S}_2$  trigonal bipyramids. (b) Projection along the 3-fold axis.

attempt to detect larger clusters above  $m/z$  300.

**Geometrical Structures.** Prominent among the questions raised by this work are those of the structures of the ions observed and the pattern of ion composition and structure. With other gaseous binary clusters there are preferred compositions (magic numbers) which can be correlated with the expansion of structural motifs.<sup>42,46,47</sup>

Our analysis has the following general tenets: (i) the structures of the gaseous  $[\text{Ni}_x\text{S}_y]^-$  ions are likely to be similar to the clusters known in condensed phases, but devoid of terminal ligands; (ii) since the number of S atoms is usually less than the number of Ni atoms, extensive bridging by the S atoms is to be expected; (iii) symmetrical, globular structures are more likely than markedly asymmetric or anisotropic shapes; (iv) Ni-Ni bonding, with Ni-Ni distances in the range 2.4–2.8 Å, is a feature common in polynickel clusters in condensed phases and is to be invoked for the gas-phase ions; (v) while smaller nickel chalcogenide clusters tend to have the chalcogenide atoms at the surface, a characteristic structural feature of the larger clusters  $[\text{Ni}_{20}\text{Te}_{18}(\text{PET}_3)_{12}]$  and  $[\text{Ni}_{34}\text{Se}_{22}(\text{PPh}_3)_{10}]$  in crystals<sup>5,9</sup> is an inner Ni/E core coated with another Ni/E layer. We note also that while many of the clusters known in crystals possess high virtual symmetry, and thus could be subject to predictions of structure from composition, others such as  $[\text{Ni}_9\text{S}_5(\text{PPh}_3)_7]^{48}$  are unusual and unpredictable.

In evaluating cluster structures we recognize the uncertainties raised by Whetten and Schriver:<sup>49</sup> "Where are the isomers?" As yet we have been able to obtain reactivity data only for the smaller  $[\text{Ni}_x\text{S}_y]^-$  ions, and only for  $[\text{Ni}_3\text{S}_3]^-$  do we have evidence for more than one ion with the one composition. For the larger ions there may be more than one structural or reactivity isomer, or the ions may be stereochemically nonrigid.

There is now an extensive literature on the electronic structures of metal clusters, including numerous successful instances of correlations of geometrical structure and valence electron population.<sup>47,50,51</sup> These correlations allow the prediction of structure

(41) Our similar investigations with copper chalcogenides yield ions up to  $m/z$  3600.<sup>23</sup>

(42) Martin, T. P. *Angew. Chem., Int. Ed. Engl.* **1986**, *25*, 197.

(43) MacMahon, T. J.; Jackson, T. C.; Freiser, B. S. *J. Am. Chem. Soc.* **1989**, *111*, 421.

(44) Sallan, L.; Lane, K. R.; Freiser, B. S. *J. Am. Chem. Soc.* **1989**, *111*, 865.

(45) Musselman, I. H.; Linton, R. W.; Simons, D. S. In *Microbeam Analysis*; Geiss, R. H., Ed.; San Francisco Press: San Francisco CA, 1985; p 337.

(46) Benedek, G.; Martin, T. P.; Pacchioni, G. *Elemental and Molecular Clusters*; Springer Verlag, 1988.

(47) Mingos, D. M. P.; Slec, T.; Zhenyang, L. *Chem. Rev.* **1990**, *90*, 383.

(48) Fenske, D.; Hachgenel, J.; Ohmer, J. *Angew. Chem., Int. Ed. Engl.* **1985**, *24*, 706.

(49) Whetten, R. L.; Schriver, K. E. In *Gas Phase Inorganic Chemistry*; Russell, D. H., Ed.; Plenum Press: New York, 1989; Chapter 6.

on the basis of electron population for clusters of transition metals coated with carbonyl or other  $\pi$ -acceptor ligands, as well as bare transition-metal and post-transition-metal clusters.<sup>47</sup> However, for heteroatom clusters of transition metals with main group elements, there are no established correlations of composition and electronic population with geometrical structure. There is ambiguity because heteroatoms can be located in the core or at the surface of a cluster, with variable participation of heteroatom valence electrons in cluster bonding. Therefore we defer questions of electronic structure and concentrate here on geometrical possibilities, thereby drawing upon the manifest structural data and principles, with the predication that gaseous  $[\text{Ni}_x\text{S}_y]^-$  clusters are de-ligated analogues of the nickel chalcogenide clusters in crystals.

Before presenting and discussing the structural possibilities, it is instructive to examine the architecture of crystalline  $\text{Ni}_3\text{S}_2$  (heazlewoodite). As shown in Figure 5, the structure is composed of  $\text{Ni}_3\text{S}_2$  trigonal bipyramids, all parallel to the crystal 3-fold axis. Each bipyramid has six Ni-S bonds, through which it is linked to six others by the formation of folded  $\text{Ni}_2\text{S}_2$  quadrilaterals. The array of eight six-connected  $\text{Ni}_2\text{S}_2$  trigonal bipyramids is almost cubic. Although the set of observed ions  $[\text{Ni}_{3x}\text{S}_{2x}]^-$ ,  $x = 1, 2, 3, 4, 5$ , could have structures composed of similarly linked  $\text{Ni}_3\text{S}_2$  trigonal bipyramids, the more highly bound structures proposed below are considered to be more probable.

The structural postulates for  $[\text{Ni}_x\text{S}_y]^-$ , labeled  $xy\text{X}$  ( $\text{X} = \text{A}, \text{B}, \text{C}, \dots$ ), are described, justified, and discussed in the following in order of increasing  $x,y$ : diagrams of most structures are presented in Chart I. The dimensions implicit in the diagrams are those observed in the large number of nickel aggregates now known, that is ca. 2.25 Å for Ni-S bonds and Ni-Ni bonds ranging from 2.4 to 3.1 Å.

$\text{Ni}_2\text{S}_2$ . The planar rhombus with Ni-Ni bonding, **22A**, is a ubiquitous constituent of many established structures and is our only postulate for this relatively stable ion.

$\text{Ni}_3\text{S}_2$ . The bicapped triangular structure **32A** ( $D_{3h}$ ) occurs in  $[\text{Ni}_3\text{S}_2(\text{PET}_3)_6]^{2+}$  and derivatives:<sup>52</sup>  $[\text{Ni}_3\text{Se}_3(\text{dppe})_3]^{2+}$ ,<sup>1b</sup>  $[\text{Ni}_3\text{S}_2(\text{Cp})_3]$ ,<sup>53</sup> and  $\text{M}_3\text{S}_2(\text{cymene})_3$ .<sup>54</sup> This is the fundamental unit of crystalline  $\text{Ni}_3\text{S}_2$  (see Figure 5).

$\text{Ni}_3\text{S}_3$ . Three structures are postulated. **33A** is a  $\text{Ni}_3$ -triangle within an  $\text{S}_3$ -triangle, probably coplanar ( $D_{3h}$ ), with three doubly bridging S atoms. In **33B** ( $C_2$ ), one S becomes triply bridging, while in **33C** ( $C_{2v}$ ) the S distribution is  $(\mu_3\text{-S})_2(\mu\text{-S})$ . **33B** can be regarded as derived from cubanoid  $\text{Ni}_4\text{S}_4$  (**44A**) by removal of one Ni-S edge, while **33C** is derived from **32A** by insertion of S into one edge of the  $\text{Ni}_3$  triangle. The reactivity data point to the existence of two different ions with the composition  $[\text{Ni}_3\text{S}_3]^-$ : the collision-induced decomposition of  $[\text{Ni}_3\text{S}_3]^-$  to  $[\text{Ni}_2\text{S}_2]^-$ ,  $[\text{NiS}_2]^-$ , and  $[\text{NiS}]^-$  can be readily envisaged as occurring from **33B** or **33C**, while the decomposition to  $[\text{NiS}_2]^-$ ,  $[\text{S}_3]^-$ ,  $[\text{S}_2]^-$ , and  $[\text{S}]^-$  could involve **33A**.

$\text{Ni}_4\text{S}_4$ . The cubanoid structure **44A** ( $T_d$ ) is well precedented, but with only one nickel chalcogenide instance  $[\text{Ni}_4\text{Se}_4(\text{PPh}_3)_4]$ .<sup>1b</sup> The alternative **44B**, a bonded  $\text{Ni}_4$  square with S bridges on all edges and all atoms coplanar ( $D_{4h}$ , cf. **33A**), is considered to be less likely.

$\text{Ni}_5\text{S}_4$ . We know of no structural precedent for a cluster with this core composition. Postulate **54A** ( $C_{2v}$ ) is based on an  $\text{Ni}_5$  square pyramid, with two  $(\mu_3\text{-S})$  caps of trans triangular faces and two  $(\mu\text{-S})$  bridges of the other basal Ni-Ni edges, and provides  $\{\text{S}_2\text{Ni}_3\}$  coordination at four Ni atoms and  $\{\text{S}_2\text{Ni}_4\}$  coordination at the fourth: the S-Ni-S coordination at each Ni is approxi-

mately linear.<sup>55</sup> Postulate **54B** ( $C_{2v}$ ) has a quite different connectivity, with  $(\mu_4\text{-S})_2(\mu_3\text{-S})_2$  bridges. This structure can be regarded as derived from **44A** by insertion of Ni across one Ni-Ni edge.

$\text{Ni}_6\text{S}_4$ . Three high-symmetry structures are postulated. In **64A** ( $T_d$ ) four faces of an  $\text{Ni}_6$  octahedron are capped by  $(\mu_3\text{-S})$ , with  $\{\text{pseudolinear S}_2 + \text{Ni}_4\}$  coordination at each Ni. The Ni-S and Ni-Ni distances are independent variables in this geometry, which like **44A** can also be viewed as a fusion of the  $\text{Ni}_3(\mu_3\text{-S})_2$  pyramids of **32A**. Structure **64B** ( $D_{3h}$ ), a body-centered trigonal prism with three  $(\mu\text{-S})$  edge bridges, is a central fragment of the framework of  $[\text{SNi}_6(\text{SBU}^1)_9]^-$ .<sup>8</sup> **64C** ( $D_{3h}$ ) is a variation of **64B** with the outer S atoms capping the square faces.<sup>56</sup>

$\text{Ni}_6\text{S}_5$ . A well-precedented structure is the fully capped trigonal prism, **65A** ( $D_{3h}$ ). Precedent exists in  $[\text{Ni}_6\text{Se}_5(\text{PPh}_3)_6]$ .<sup>57</sup> While **65A** maximizes bonding opportunities and provides each Ni with  $\{\text{Ni}_3 + \text{trigonal S}_3\}$  coordination, structural isomers derived by fluxions with minimal bond disruption can be envisaged. By a twist of one pyramidal cap about the 3-fold axis the  $\text{Ni}_6$  is converted to an octahedron, with five  $(\mu_3\text{-S})$  caps, **65B** ( $C_{3v}$ ): this process involves breaking only three Ni-S bonds. The alternative **65C** ( $D_{3h}$ ), in which the three equatorial S atoms bridge edges rather than faces of the  $\text{Ni}_6$  trigonal prism, is considered less likely as it further reduces the degree of Ni coordination by S. Other  $\text{Ni}_6$  polyhedra, such as the bicapped tetrahedron, possess too many faces for effective bridging by five S atoms.

$\text{Ni}_7\text{S}_5$ . A symmetrical structure, **75A** ( $D_{3h}$ ), is derived from nickel-centered **65A**. This centering has geometrical consequences: the central Ni must expand the trigonal prism to the extent that the rectangular faces expand to ca.  $3.0 \times 3.4$  Å, which are very weak Ni-Ni bonds, and then the S atom capping each such face must be located too close ( $<2.0$  Å) to the central Ni if the Ni-S capping bonds are to be reasonable lengths of 2.3 Å. Therefore the bonding in **75A** is as shown. The closest precedent for this structure type occurs in the crystal structure of  $[\text{Ni}_6\text{S}_5(\text{PPh}_3)_7]$ ,<sup>48</sup> in which there is an additional equatorial Ni atom. Pentagonal bipyramidal  $\text{Ni}_7$  frameworks are not readily elaborated as structures for  $\text{Ni}_7\text{S}_5$  or  $\text{Ni}_7\text{S}_6$ .

$\text{Ni}_7\text{S}_6$ . Structure **76A** ( $C_{3v}$ ) is best regarded as derived from the cubic  $\text{Ni}_8$  plus octahedral  $\text{S}_6$  structure of (**86A**) by removal of one Ni vertex and partial closing of the large  $\text{Ni}_3$  triangular face so created. The three quadrilateral faces and the three smaller triangular faces are capped by S. There is precedent for this structure type in  $[\text{Co}_7\text{S}_6\text{Cl}_2(\text{Ph}_3\text{P})_5]$ ,<sup>48</sup>  $[\text{Co}_7\text{S}_6\text{Cl}_3(\text{PPh}_3)_4]$ ,<sup>1b</sup> and  $[\text{Fe}_7\text{S}_6\text{Cl}_3(\text{PET}_3)_4]$ .<sup>58</sup> There is dimensional freedom in **76A** and all Ni-Ni and Ni-S bonds can take standard values.

$\text{Ni}_8\text{S}_5$ . There are four regular  $\text{M}_8$  frameworks, the cube, the triangular dodecahedron, the ditetrahedron (also called the tetra-capped tetrahedron, the stella quadrangular, or tetraederstern<sup>59</sup>), and the bicapped trigonal prism. These have at least six faces, and thus fully S-capped structures are not possible for the composition  $\text{Ni}_8\text{S}_5$ . The postulated structure **85A** ( $C_{2v}$ ) is based on the crystal structure of  $[\text{Ni}_8\text{S}_5(\text{PPh}_3)_7]$ ,<sup>48</sup> without its terminal ligands. The Ni framework is a centered trigonal prism with one equatorial Ni: some distortion from this ideal is necessary to allow the Ni-S and Ni-Ni distances to take reasonable values.

$\text{Ni}_8\text{S}_6$ . High symmetry can occur here in **86A** ( $O_h$ ) containing the Platonic cube and octahedron. All dimensions can be idealized. There is precedent for this core structure in crystals of  $[\text{Ni}_8\text{S}_6\text{Cl}_2(\text{PPh}_3)_6]$ <sup>48</sup> and  $[\text{Ni}_8\text{S}_6(\text{PPh}_3)_6]$ .<sup>1b</sup> A slightly less symmetric isomer of **86A** is **86B** ( $T_d$ ), in which the eight Ni atoms

(50) Lauher, J. W. *J. Am. Chem. Soc.* **1978**, *100*, 5305.

(51) (a) Mingos, D. M. P. *Acc. Chem. Res.* **1984**, *17*, 311. (b) Mingos, D. M. P. *J. Chem. Soc., Chem. Commun.* **1985**, 1352. (c) Mingos, D. M. P.; Johnston, R. L. *Struct. Bonding* **1987**, *68*, 29. (d) Wales, D. J.; Mingos, D. M. P.; Slee, T.; Zhenyang, L. *Acc. Chem. Res.* **1990**, *23*, 17.

(52) Ceccconi, F.; Ghilardi, C. A.; Midollini, S.; Orlandini, A.; Vacca, A.; Ramirez, J. A. *J. Chem. Soc., Dalton Trans.* **1990**, 773.

(53) Vahrenkamp, H.; Uchtman, V. A.; Dahl, L. F. *J. Am. Chem. Soc.* **1968**, *90*, 3272.

(54) Lockemeyer, J. R.; Rauchfuss, T. B.; Rheingold, A. L. *J. Am. Chem. Soc.* **1989**, *111*, 5733.

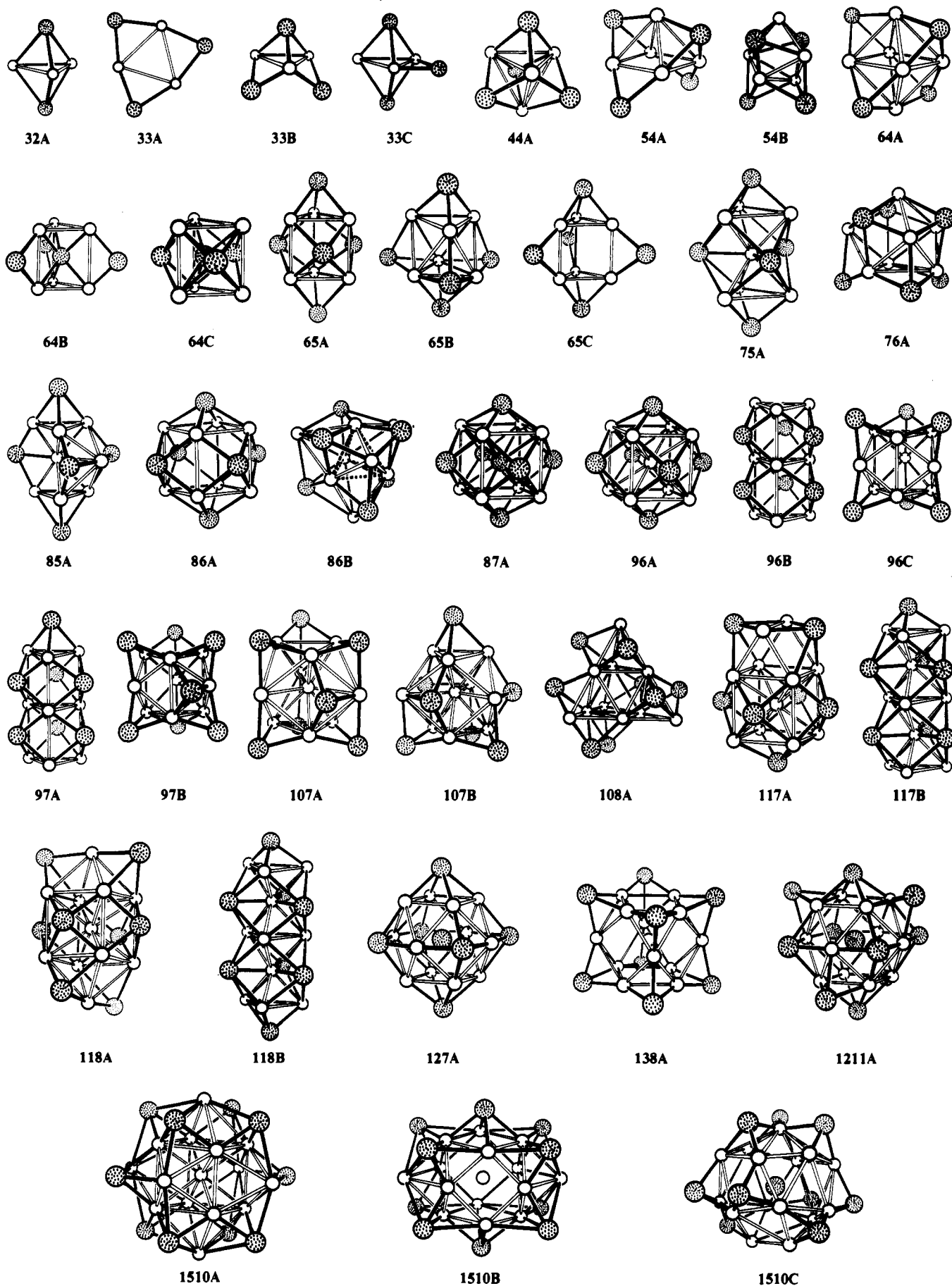
(55) We exclude the  $C_{4v}$  structure in which a square pyramid  $\text{Ni}_4$  has four  $(\mu_3\text{-S})$  caps, because it contains disproportionate Ni coordination, namely one Ni with approximately square  $[\text{S}_4]$  coordination, and four Ni with angular ( $<90^\circ$ )  $[\text{S}_2]$  coordination.

(56) (a) The crystalline compound  $[\text{Ni}_6\text{Se}_4(\text{MeCp})_5]^{56b}$  has  $\text{Ni}_4$  and  $\text{Ni}_3$  fragments linked at a spiro Ni atom and is considered to be an improbable model for  $[\text{Ni}_6\text{S}_4]^-$ . (b) Fenske, D.; Hollnagel, A. *Angew. Chem., Int. Ed. Engl.* **1989**, *28*, 1390.

(57) Fenske, D.; Ohmer, J. *Angew. Chem., Int. Ed. Engl.* **1987**, *26*, 148.

(58) Noda, I.; Snyder, B. S.; Holm, R. H. *Inorg. Chem.* **1986**, *25*, 3851.

(59) Zheng, C.; Hoffmann, R.; Nelson, D. R. *J. Am. Chem. Soc.* **1990**, *112*, 3784.

Chart I. Diagrams of Structural Postulates for Ions  $[\text{Ni}_x\text{S}_y]^-$ , Labeled  $xyX$  ( $X = \text{A, B, C, ...}$ )<sup>a</sup>

<sup>a</sup>Ni-S bonds are drawn filled, Ni-Ni connections within bonding range ( $<2.9 \text{ \AA}$ ) are marked as open bonds, except in **86B** where the inner tetrahedron is differentiated as broken bonds and larger structures where bonds to the central atom are omitted to clarify the diagrams.

constitute a ditetrahedron: **86B** derives from **86A** by inversion of four of the Ni atoms through their triangular faces of the  $S_6$  octahedron. This creates another six internal Ni-Ni bonds. In this structure all Ni-Ni bonds are 2.7 Å, while each S is bonded to two Ni atoms at 2.2 Å and two at 2.5 Å.

$Ni_8S_7$ . Structure **87A** ( $O_h$ ) is S-centered **86A**. The central S-Ni distance (2.4 Å) and the Ni-Ni distance (2.7 Å) are normal, and the capping S-Ni distance is unconstrained except by close contact between central and capping S atoms (S-S = 2.5 Å when Ni-S = 2.25 Å). A recent extended Huckel molecular orbital calculation<sup>60</sup> indicates that the homologous  $Ni_8Te_7$  core with structure **87A** would be stabilized by bonding interactions between the central ( $\mu_8$ -Te) and the Ni and ( $\mu_4$ -Te) atoms.

$Ni_9S_6$ . Four symmetrical  $M_9$  cluster frameworks can be considered, namely (i) the metal-centered cube (known in  $[Ni_9Te_6(PEt_3)_8]$ ,<sup>9,60</sup>  $[Ni_9(\mu_4-As)_6(PPh_3)_3Cl_3]$ ,<sup>61</sup> and  $[Pd_9As_6(PPh_3)_8]$ <sup>62</sup>), (ii) a pair of confacial octahedra (the dioctahedron, which occurs in  $[Ni_9S_9(PEt_3)_6]^{2+2}$  and  $[Co_9Se_{11}(PPh_3)_6]$ ,<sup>63</sup> (iii) a pair of trigonal prisms sharing a triangular face (the trigonal diprism) which is a fragment of the crystal structure of Millerite (see below), or (iv) the tricapped trigonal prism.

An obvious structure for  $Ni_9S_6$  is **96A** ( $O_h$ ), the metal centered cube with six ( $\mu_4$ -S) caps, in which the Ni-Ni distances are 2.45 or 2.8 Å, while the Ni-S distances are 2.25 or (center to cap) 2.5 Å. High symmetry alternative postulates are **96B** ( $D_{3h}$ ), the trigonal diprism with square faces capped by sulfide, and **96C** ( $D_{3h}$ ), in which there are six ( $\mu_3$ -S) caps on triangular faces of the tricapped trigonal prism, with all distances unconstrained. Structures based on the dioctahedron are not postulated because more than six bridging sulfide ligands would be required.

$Ni_9S_7$ . Structures **97A** ( $C_{3v}$ ) and **97B** ( $C_3$ ) are derived from **96B** and **96C**, respectively, by addition of one ( $\mu_3$ -S) cap with unconstrained Ni-S distances.

$Ni_{10}S_7$ . Apart from some gold clusters and the tetraadamantanoid clusters  $[E_4Cd_{10}(SR)_{16}]^{4-20}$   $M_{10}$  frameworks are uncommon in metal cluster chemistry. We postulate the metal-centered tricapped trigonal prism and the tetraadamantanoid frameworks as the likely symmetrical metal arrays for the  $Ni_{10}$  sulfide cluster ions. The  $Ni_8$  framework in the known structure of  $[Ni_8S_5(PPh_3)_7]$ <sup>48</sup> (embodied in **85A**) is in fact the metal-centered tricapped trigonal prism without two of the equatorial Ni atoms.

For  $Ni_{10}S_7$  we propose the metal-centered tricapped trigonal prism, which allows isomeric distributions of the seven ( $\mu_3$ -S) caps. The two isomers considered most likely are **107A** ( $C_3$ ) and **107B** ( $C_{3v}$ ). With use of geographical imagery, **107A** has six "tropical" caps and one "equatorial" cap, while **107B** has one "polar" cap, three "equatorial" caps, and three "tropical caps". The atom array in **107A** is in effect the Ni-centered version of **97B**, but the Ni-Ni distances and bonding are necessarily different.

$Ni_{10}S_8$ . The tetrahedral tetraadamantanoid  $Ni_{10}$  framework has a total of 16  $Ni_3$  triangles over its four faces. Postulate **108A** ( $C_1$ ) has regular placement of eight ( $\mu_3$ -S) caps, such that each of the four outer Ni atoms has irregular  $\{(\mu_3-S)_2Ni_3\}$  coordination, while the six others have irregular  $\{(\mu_3-S)_3Ni_6\}$  coordination. Another postulate (not drawn) is **108B** ( $D_{3h}$ ), which is **107A** with a ( $\mu_3$ -S) cap added in an axial position.

$Ni_{11}S_7$ . Two proposals are made. The more globular is **117A** ( $C_{2v}$ ), which displays structural elements present in **65A** and **96A**. The alternative, **117B** ( $C_{3v}$ ), is generated by stacking two of the metal-centered trigonal prisms of **75A**. Both are acceptable but unprecedented.

$Ni_{11}S_8$ . The two postulates are analogous to those described in the previous paragraph. **118A** ( $D_{2d}$ ) is a derivative of **96A**, while **118B** ( $D_{3h}$ ) is a derivative of **75A**.

$Ni_{12}S_7$ . Symmetrical  $Ni_{12}$  polyhedra are the icosahedron, the cuboctahedron, and the anticuboctahedron. With 20 equivalent faces the icosahedron cannot be symmetrically capped with the 7, 8, or 11 S atoms in the observed ions, and therefore in the following we develop cuboctahedral  $Ni_{12}$  structures.

For  $Ni_{12}S_7$  the highest symmetry structure is **127A** ( $O_h$ ), the S-centered  $Ni_{12}$  cuboctahedron with ( $\mu_4$ -S)<sub>6</sub> over the square faces of the cuboctahedron. The center to vertex distances of a cuboctahedron equal the edge lengths, and therefore in idealized **127A** the  $S^{central}$ -Ni bond lengths and the Ni-Ni bond lengths are equal. This is not unreasonable since  $S^{central}$  is 12 coordinate and therefore would be expected to have unusually long bonds. It is possible for **127A** to distort to shorten some of the  $S^{central}$ -Ni bonds. The capping Ni-S bond lengths are independently variable.

$Ni_{12}S_8$ . Again a high-symmetry structure is possible, namely **128A** ( $O_h$ , not drawn, but equivalent to **138A** without the central Ni), in which an  $Ni_{12}$  cuboctahedron has ( $\mu_3$ -S)<sub>8</sub> caps over the triangular faces. The Ni-Ni distances and the Ni-S distances are independently variable. There is precedent in the crystalline  $[M_{12}S_8]^{4-}$  clusters, M = Cu,<sup>64</sup> Au.<sup>65</sup>

$Ni_{12}S_{11}$ . One postulate is an S-centered  $Ni_{12}$  cuboctahedron capped by sulfide on 10 of its 14 faces, as in **1211A** ( $T_d$ ): lower symmetry capping isomers are possible. An alternative structure, **1211B** ( $D_{3h}$ , not drawn, but compare **97A**), is a column of three trigonal prisms, fully capped on the nine square faces and the two end triangular faces. There is precedent for columnar trigonal prisms in the crystal structure of NiS (millerite, see below). In crystalline molecular compounds there exist columnar metal chalcogenide clusters based on confacial octahedral, but all of these have a larger number of chalcogenide atoms: examples are  $[Ni_{12}Se_{12}(PEt_3)_6]^{57}$  and  $[Mo_{12}Se_{14}]^{2-17}$

$Ni_{13}S_8$ . The high-symmetry structure is **138A** ( $O_h$ ), an Ni-centered cuboctahedron, with ( $\mu_3$ -S)<sub>8</sub> over the triangular faces. This is Ni-centered **128A**. Precedent for M-centered 12-hedra abounds in bulk metals and in metal carbonyl clusters. The low S/Ni ratio in this ion means that alternative columnar Ni frameworks could not be adequately encompassed by S caps.

$Ni_{15}S_{10}$ . The  $Ni_{15}Se_{10}$  composition occurs in two very similar crystalline clusters,  $[Ni_{15}Se_{10}(CO)_3(MeCp)_8]$  and  $[Ni_{15}Se_{10}(CO)Cl_2(MeCp)_8]$ .<sup>56b</sup> However the frameworks of these involve protruding Ni atoms that are capped by the Cp ligands. This structural feature does not occur in any other cluster and is inappropriate for gas-phase clusters devoid of terminal ligands. The metal frameworks in metal carbonyl clusters with >13 M atoms are based on capped 12-hedra, as occur in the carbonyl clusters  $[Rh_{15}(CO)_{27}]^{3-66}$  and  $[Rh_{17}(CO)_{30}]^{3-67}$ . However these metal cores require many terminal ligands: with a deficiency of ligands in  $Ni_{15}S_{10}$ , more equitable bonding is achieved with S caps on the square faces rather than M capping the square faces. Therefore we pursue other architectural motifs.

One postulate, inspired by the structure of crystalline  $[Rh_{14}(CO)_{25}]^{4-66}$  is **1510A** ( $D_{2h}$ ) in which the  $Ni_{15}$  core is an Ni-centered rhombic dodecahedron. Alternatively this core is recognized as a Ni-centered cube with Ni caps on all faces. To maintain suitable Ni-Ni distances within the core, the 12 quadrilateral faces are likely to be folded about their shorter diagonals, and it is across these that capping S atoms have their shorter Ni-S bonds: two of these faces are not S-capped. In the variant **1510B** there is a Ni-centered  $Ni_{12}$  cuboctahedron.

We note also that a symmetrical and approximately spherical  $M_{15}$  array occurs in  $[ClV_{15}O_{36}]^{5-,68,69}$  with a monatomic ligand atom at the center. In **1510C** ( $C_1$ ) we propose a structure for  $[Ni_{15}S_{10}]^-$  using nine ( $\mu_3$ -S) caps and a central S atom.

(64) Betz, P.; Krebs, B.; Henkel, G. *Angew. Chem., Int. Ed. Engl.* **1984**, *23*, 311.

(65) Marbach, G.; Strahle, J. *Angew. Chem., Int. Ed. Engl.* **1984**, *23*, 715.

(66) Martlengo, S.; Ciani, G.; Chini, P.; Sironi, A. *J. Am. Chem. Soc.* **1978**, *100*, 7096.

(67) Ciani, G.; Magni, A.; Sironi, A.; Martlengo, S. *J. Chem. Soc., Chem. Commun.* **1981**, 1280.

(68) Müller, A.; Krickemeyer, E.; Penk, M.; Walberg, H.-J.; Bögge, H. *Angew. Chem., Int. Ed. Engl.* **1987**, *26*, 1045.

(69) Pang, T.; Dance, I. G.; Craig, D. C.; Scudder, M. L. In preparation.

(60) Wheeler, R. A. *J. Am. Chem. Soc.* **1990**, *112*, 8737.

(61) Fenske, D.; Merzweiler, K.; Ohmer, J. *Angew. Chem., Int. Ed. Engl.* **1988**, *27*, 1512.

(62) Fenske, D.; Fleischer, M.; Persau, C. *Angew. Chem., Int. Ed. Engl.* **1989**, *28*, 1665.

(63) Fenske, D.; Ohmer, J.; Hachgenei, J. *Angew. Chem., Int. Ed. Engl.* **1985**, *24*, 993.

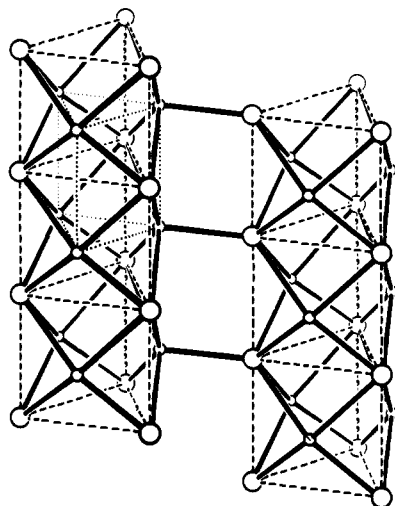


**Figure 6.** Representation of part of the crystal structure of Millerite, NiS, showing the columns of stacked  $S_6$  trigonal prisms and  $Ni_6$  trigonal prisms and the connections between them: small circles are Ni atoms.

A third structure type for  $Ni_{15}S_{10}$  could be derived from five  $Ni_3S_2$  trigonal bipyramids, edge linked as in crystalline  $Ni_3S_2$ : the tempting notion of  $Ni_{15}S_{10}$  as a trigonal bipyramid of trigonal bipyramids encounters geometrical difficulties at central bridging atoms. The connectivity and thus rigidity of linked  $Ni_3S_2$  trigonal bipyramids would be substantially less than the other structure postulates and is discounted for this reason.

All of the structures postulated above are consistent with the local and global structural principles manifest in established compounds. The S-capped  $Ni_3$  triangles, S-capped  $Ni_4$  rhombuses, and S-capped  $Ni_4$  squares are well-precedented features. We note that the Ni-centered cuboctahedron in **138A** and **1510B** is a fragment of the structure of metallic nickel. Further, the  $Ni_6$ -trigonal prism with ( $\mu_4$ -S) capping the rectangular faces, occurring in postulated structures **65A**, **75A**, **96B**, **97A**, and **1211B**, is the principal structural unit of another of the crystal structures of nickel sulfide, NiS, Millerite.<sup>70,71</sup> Figure 6 shows that the trigonal prisms are stacked along their 3-fold axes and that the structure can also be analyzed as stacked trigonal prisms  $S_6$  with Ni-capped rectangular faces: all trigonal columns are linked by Ni-S bonds.

(70) Grice, J. D.; Ferguson, R. B. *Can. Mineral.* **1974**, *12*, 248.

(71) Rajamani, V.; Prewitt, C. T. *Can. Mineral.* **1974**, *12*, 253.

The tricapped trigonal prism occurs also in  $(\eta^3-C_4H_7)_6Pd_6Se_3$ .<sup>72</sup>

### Conclusions

A rich set of negative ions  $[Ni_xS_y]^-$  can be obtained by laser ablation of nonmolecular solid nickel sulfides. It is probable that these ions are formed in the laser-induced plasma at the sample surface, and therefore the ions do not directly reflect the composition of the solid sample: there is no evidence from this investigation that laser ablation is able to preferentially excise molecular fragments from the solid, and thus fulfill the first of the expectations in the introduction. This result is consistent with our  $^{252}Cf$  plasma desorption mass spectrometry of solid cadmium thiolates, where again the observed ions do not match fragments expected from knowledge of the nonmolecular solid-state structures.<sup>73,74</sup> The smaller of the  $[Ni_xS_y]^-$  ions vary substantially in their reactivities: we hope to be able to increase the sensitivity of our experiments in order to investigate the reactivities of the larger ions.

The compositions of the  $[Ni_xS_y]^-$  ions bear broad correspondence with the cores of known nickel chalcogenide clusters in condensed phases, and accordingly we have based our postulated structures for the ions on precluded structures and established principles. Structural isomerism, and fluxionality of the Ni frameworks and of the S-capping connections, is possible in many of the proposed structures. It is logical to conclude, simply from the compositions of all ions, that the cores that appear in condensed-phase structures with terminating ligands can exist in the gas phase without the terminating ligands. We are undertaking various theoretical approaches to the structures of these ions, including the calculation and minimization of the total energies using models with atom-pair electrostatic interactions and Born-Mayer interatomic repulsions.<sup>42,75,76</sup>

**Acknowledgment.** This research is supported by the Australian Research Council (I.G.D., G.D.W.). K.J.F. acknowledges the award of a National Research Fellowship. We thank Mr. D. Craig for programming assistance.

Registry No.  $Ni_3S_2$ , 12035-72-2; NiS, 16812-54-7.

(72) Fenske, D.; Hollnagel, A.; Merzweiler, K. *Z. Naturforsch.* **1968**, *43b*, 634.

(73) Craig, A. G.; Kamensky, I.; Garbutt, R. G.; Dance, I. G.; Derrick, P. J. *Int. J. Mass Spectrom. Ion Proc.* **1988**, *86*, 273.

(74) Craig, A. G.; Dance, I. G.; Derrick, P. J. *J. Am. Chem. Soc.* In preparation.

(75) (a) Martin, T. P.; Kakizaki, J. *Chem. Phys.* **1984**, *80*, 3956. (b) Diefenbach, J.; Martin, T. P. *Surf. Sci.* **1985**, *156*, 234. (c) Martin, T. P. *Adv. Solid State Phys.* **1984**, *24*, 1.

(76) Yu, W.; Freas, R. B. *J. Am. Chem. Soc.* **1990**, *112*, 7126.